PHOTONICS Research

Low-latency full-field temporal magnification based on spectral compression

Xiangzhi Xie,[1] Jilong Li,[2] Feifei Yin,[1] Kun Xu,[1] and Yitang Dai[1,*]

[1]State Key Laboratory of Information Photonics and Optical Communications, Beijing University of Posts and Telecommunications, Beijing 100876, China
[2]Advanced Institute of Photonics Technology, School of Information Engineering, and Guangdong Provincial Key Laboratory of Information Photonics Technology, Guangdong University of Technology, Guangzhou 510006, China
*Corresponding author: ytdai@bupt.edu.cn

Received 5 August 2021; revised 18 October 2021; accepted 20 October 2021; posted 21 October 2021 (Doc. ID 438498); published 23 November 2021

Temporal magnification is an emerging technology for the observation of single-shot optical signals with irregular and ultrafast dynamics, which exceed the speed, precision, and record length of conventional digitizers. Conventional temporal magnification schemes suffer from transmission delay and large volume of dispersive elements. Because only the signal envelope can be magnified in the dispersion-based schemes, real-time full-field (phase and amplitude) measurement for a complex ultrafast optical signal remains an open challenge. Here, a bandwidth-compressed temporal magnification scheme for low-latency full-field measurements of ultrafast dynamics is proposed. Unlike the dispersion-based schemes, temporal magnification of a complex optical signal is achieved by bandwidth compression. The bandwidth is coherently compressed by the Vernier effect relying on the detuned free spectral range of a periodic optical filter and time lens. Experimentally, a temporal magnification factor of 224 is realized, and full-field measurements for picosecond pulses are demonstrated. The proposal eliminates the dependence on dispersive elements and shows great potential in integration, which may pave a new path toward full-field measurement for nonrepetitive and statistically rare signals.

https://doi.org/10.1364/PRJ.438498

1. INTRODUCTION

Real-time measurements for optical signal that have irregular and ultrafast dynamics over a large time-scale require a high temporal resolution that exceeds the speed and capacity of a conventional digital signal processor. Extensive efforts have been directed to the realization of photonics-assisted methods, which are used to slow down the ultrashort events and overcome the speed limitation of electronic digitizers. The photonics-assisted methods have achieved remarkable success in the observation of transient phenomena in recent years [1–11]. Temporal magnification is one of the most outstanding photonics-assisted schemes for the measurement of rare nonstationary events, where the duration of a signal envelope is greatly stretched [12]. A typical temporal magnification system consists of a time lens and dispersive elements [13]; the signal is prestretched by the first dispersive element and then pre-chirped by the time lens to acquire a temporal quadratic phase; finally, the envelope of an optical signal is magnified after propagation in the second dispersive element. The sampling rate of an analog-to-digital converter (ADC) can be effectively improved by temporal magnification [14–18]. Because the duration of an ultrashort nonstationary signal is greatly extended, continuous measurements can be realized. The inherent physics of transient phenomena, such as optical rouge waves [2–4], soliton dynamics [8], and supercontinuum [11], have been well explored by the temporal magnification method.

Low latency is a critical requirement in the capture of ultrafast dynamics, which can effectively avoid information loss in the analysis process. Unfortunately, the propagation delay introduced by dispersive elements may impair real-time performance of the observation. In addition, the complete picture of a variety of fundamental phenomena needs to be drawn with both phase and amplitude, while the dispersion-based schemes only focus on magnification of the signal envelope. The realization of large temporal magnification ratio is dependent on large dispersive elements. Only the optical fiber is the suitable dispersion medium for the magnification of a broadband optical signal, while the accompanying transmission delay inevitably affects the system's real-time performance. For example, a spool of dispersion compensation fiber (DCF) with dispersion of −2720 ps/nm is employed in Ref. [16], where the transmission delay is around hundreds of microseconds.

Moreover, real-time phase measurement remains an open challenge in conventional dispersion-based schemes. The secondary

phase distortion caused by dispersion cannot be avoided in principle. Additional digital signal processing (DSP) is necessary for the recovery of phase, where the processing delay greatly limits the analysis speed and makes it not competitive in the capture of ultrafast dynamics. In Ref. [8], the simultaneous use of temporal magnification and dispersive Fourier transform enables the recording of the envelope and spectrum of the signal at the same time. The Gerchberg–Saxton algorithm is addressed to recover the optical phase from time-domain and frequency-domain measurements [19]. The reconstruction of the amplitude and phase provides insight into the ultrafast dynamics in optics. However, the digital signal processing delay may become an obstacle to the continuous observations of irregular signals. In Ref. [9], soliton dynamics in optical microcavities are observed by optical sampling and electric-field cross-correlation, while it is targeted at the measurements of quasi-periodic signals.

In this paper, a dispersion-free real-time full-field measurement scheme is proposed, and the characterization for a variety of transient complex optical signals is experimentally demonstrated. Unlike the dispersion-based methods, this solution takes advantage of bandwidth compression to achieve temporal magnification. The bandwidth compression relies on the Vernier effect, where the free spectral range (FSR) of the periodic optical filter and time lens is slightly detuned. The bandwidth compression is divided into two steps: the optical signal under test is spectrally sampled by a periodic optical filter; then, the discrete spectral components are injected into a time lens and optical waveshaper, which brings different spectral components together and coherently compresses the signal bandwidth. Fortunately, the optical phase is preserved during the bandwidth compression, which enables the recovery of the phase information without relying on complex algorithms. Experimentally, real-time measurements for picosecond optical pulses with a complex envelope are demonstrated, where both phase and amplitude are well recovered. Because the proposal eliminates the dependence on dispersion elements, an integrated temporal magnification system could be expected in this method.

2. PRINCIPLE

Our proposal uses coherent temporal magnification to realize the observation of an ultrafast transient signal. Compared with the conventional temporal magnification method, our proposal no longer requires a dispersion medium and can achieve the coherent temporal magnification (both phase and amplitude). The configuration of the conventional temporal magnification scheme is shown in Fig. 1(a). The magnification of the temporal waveform can be achieved if $1/D_1 + 1/D_2 = 1/D_f$ is satisfied and the magnification factor is determined by the ratio between the first and second dispersion value [13]. The configuration of the proposed system is shown in Fig. 1(b). The temporal magnification is achieved by spectral compression, which eliminates dependence on dispersion. Both amplitude and phase information of the input signal can be detected. The processing latency (~10 ns) is only limited by the transmission delay in the optical device, which can be estimated by the time-bandwidth of the filter and the length of optical path. The spectral compression is composed of two components: spectral sampling and time lens. The broadband input spectrum [Fig. 1b(1)] is sampled by a Vernier comb filter (VCF). Then, the discrete spectral components [Fig. 1b(2)] are injected into a time lens, which enables the convergence of spectral components. The frequency response of the time lens is a periodic frequency impulse function with free spectral range (FSR) of $\mathrm{FSR_{TL}}$. The focal group delay dispersion (GDD) of the time lens is compensated by an optical waveshaper. Because the FSR of the VCF and time lens is slightly mismatched, the original large frequency interval of the spectral components

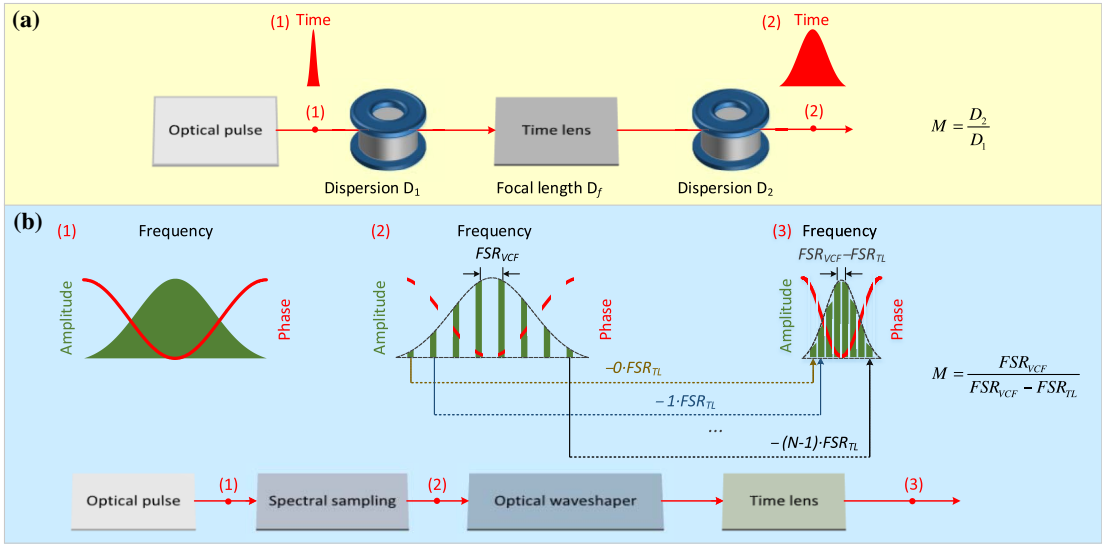

Fig. 1. (a) Configuration of the conventional temporal magnification scheme. D_1, D_2 are the dispersion values of the first and second dispersive elements, respectively. D_f is the focal length of the time lens. Magnification factor M can be expressed as D_2/D_1. (b) Structure of the proposed temporal magnification scheme. $\mathrm{FSR_{VCF}}$ and $\mathrm{FSR_{TL}}$ represent the FSR of Vernier comb filter (VCF) and time lens, respectively. The bandwidth compression is achieved by Vernier effect, where $\mathrm{FSR_{VCF}}$ is slightly larger than $\mathrm{FSR_{TL}}$. Magnification factor M can be expressed as $\mathrm{FSR_{VCF}}/(\mathrm{FSR_{VCF}} - \mathrm{FSR_{TL}})$.

is compressed into a relatively narrow band [Fig. 1b(3)]. The spectral sampling and propagation in the time lens preserve the initial phase information. The ultrafast transient signal can be recovered without extra-complex algorithms.

The spectral compression is equivalent to the magnification of a temporal waveform, which can be expressed as

$$X_{\text{out}}(M\omega) = X_{\text{in}}(\omega) \Leftrightarrow \frac{1}{M} x_{\text{out}}\left(\frac{t}{M}\right) = x_{\text{in}}(t). \tag{1}$$

Here, X_{out} and X_{in} represent the spectra of the input and output signal, x_{out} and x_{in} are the temporal expressions of the input and output signal, and M is the ratio of bandwidth compression. As Eq. (1) shows, the magnification factor of the temporal waveform is equal to the ratio of spectral compression, which is composed of spectral sampling and a dispersion-compensated time lens. The spectral sampling of the broadband input signal is realized by VCF with FSR of FSR_{VCF}. The sampled spectrum, $Y(\omega)$, after the VCF can be expressed as

$$\begin{aligned} Y(\omega) &= X_{\text{in}}(\omega) \cdot \sum_k H(\omega - k \cdot 2\pi \text{FSR}_{\text{VCF}}) \\ &\approx \sum_k A_k e^{j\varphi_k} H(\omega - k \cdot 2\pi \text{FSR}_{\text{VCF}}), \end{aligned} \tag{2}$$

where $H(\omega - k \cdot 2\pi\text{FSR}_{\text{VCF}})$ represents the kth transmission peak of VCF. Assuming the amplitude and phase response within the transmission peak are constant, they are denoted by A_k and $e^{j\varphi_k}$, respectively. Output of the kth transmission peak can be approximated as $A_k e^{j\varphi_k} H(\omega - k \cdot 2\pi\text{FSR}_{\text{VCF}})$, as shown in Eq. (2). The time lens is generated by electro-optic modulation, where the RF signal driving the phase modulator is sinusoidal. The time lens is realized by cascaded electro-optic modulators [12]. The focal GDD is compensated by an optical waveshaper. The bandwidth of time lens can be extended by improving the power of driving signal and increasing the number of the cascaded modulators. The frequency impulse response of the dispersion-compensated time lens, $\text{TL}(\omega)$, can be described as

$$\text{TL}(\omega) = \sum_m \delta(\omega - m \cdot 2\pi \text{FSR}_{\text{TL}}), \tag{3}$$

where m represents the number of impulse responses. The discrete spectral components are mixed with a plurality of local oscillation signal from the time lens. From the view of frequency domain, output of the optical waveshaper is the convolution between the discrete spectral components and the frequency impulse sequence. The output spectrum can be illustrated as follows:

$$\begin{aligned} &Y(\omega) \otimes \text{TL}(\omega) \\ &\quad = \sum_k A_k e^{j\varphi_k} \sum_m H[\omega - k \cdot 2\pi \text{FSR}_{\text{VCF}} - m \cdot 2\pi \text{FSR}_{\text{TL}}]. \end{aligned} \tag{4}$$

Equation (4) suggests that the frequency interval of the spectrum gathering position is FSR_{VCF}; thus, the compressed bandwidth should be less than FSR_{VCF} to avoid spectrum overlap. Bandpass optical filtering is employed to filter out the spectral components, which satisfy $k = -m$. The frequency interval of spectral components is compressed after mixing with the frequency impulse sequence. The compressed spectrum, $X_{\text{out}}(\omega)$, can be written as

$$\begin{aligned} X_{\text{out}}(\omega) &= \sum_k A_k e^{j\varphi_k} H[\omega - k \cdot 2\pi(\text{FSR}_{\text{VCF}} - \text{FSR}_{\text{TL}})] \\ &\approx X_{\text{in}}\left(\frac{\text{FSR}_{\text{VCF}} - \text{FSR}_{\text{TL}}}{\text{FSR}_{\text{VCF}}} \omega\right). \end{aligned} \tag{5}$$

Frequency of the kth component is decreased by $(k-1)\text{FSR}_{\text{TL}}$. The original frequency interval of FSR_{VCF} is compressed into $\text{FSR}_{\text{VCF}} - \text{FSR}_{\text{TL}}$. The ratio of bandwidth compression can be written as $(\text{FSR}_{\text{VCF}} - \text{FSR}_{\text{TL}})/\text{FSR}_{\text{VCF}}$. The maximum of bandwidth compression ratio is determined by the quality factor of the VCF. The temporal magnification factor, M, is inversely proportional to bandwidth compression ratio, which can be expressed as

$$M = \frac{\text{FSR}_{\text{VCF}}}{\text{FSR}_{\text{VCF}} - \text{FSR}_{\text{TL}}}. \tag{6}$$

The operation bandwidth of the proposed system is mainly determined by the convergence ability of the time lens to different frequency components. The operation bandwidth of the system is written as $N \cdot \text{FSR}_{\text{VCF}}$, where N is the number of the frequency impulses of the time lens. According to the Nyquist sampling law, when the spectral sampling rate is larger than the duration of input signal, the sampling process will not lose information. The spectral sampling rate should satisfy

$$\text{FSR}_{\text{VCF}} \le \frac{1}{\tau}, \tag{7}$$

where τ represents the duration of input signal. The spectral sampling interval needs to be customized for the duration of signal to be tested.

An optical loss is introduced by the spectral sampling and insertion loss of VCF. The loss of spectral sampling can be estimated by the sampling duty cycle and shape of the sampling function. Because the signal and noise are simultaneously filtered, the signal-to-noise ratio (SNR) is not deteriorated. The SNR is mainly affected by the insertion loss of VCF (around 4 dB). An optical amplifier is employed to compensate the optical loss of the sampling process, which contributes to the maintenance of sensitivity after propagation in subsequent optical devices.

The compressed spectrum is formed by the coherent synthesis of multiple frequency components with a discretization step of $\text{FSR}_{\text{VCF}} - \text{FSR}_{\text{TL}}$. Because the compressed spectrum is not continuous, the output waveform is also affected by the discretization step and shape of each discrete component. The discretization step determines the repetition rate of output pulses, and the shape of sampling function affects the envelope of the output pulse sequence. In order to avoid the interference between the spectral components, the discretization step of the compressed spectrum is set to be larger than the 3 dB bandwidth of transmission peak. Mathematically, the output discrete spectral components are expressed as $\sum_k A_k e^{j\varphi_k} H\{[\omega - k \cdot 2\pi(\text{FSR}_{\text{VCF}} - \text{FSR}_{\text{TL}})]\}$. Actually, the periodic spectral components are corresponding to a sequence

of periodic temporal pulse. The temporal output can be obtained through inverse Fourier transform. Duration of the pulse sequence can be estimated by the 3 dB bandwidth of $H(\cdot)$.

3. EXPERIMENTAL RESULTS

The experimental setup of the proposed dispersion-free temporal magnification scheme is illustrated in Fig. 2. The programmable laser is used to generate an ultrafast optical signal with specific amplitude and phase characteristics. The programmable laser is composed of a femtosecond laser, an MZM, and an optical waveshaper (Finisar, WaveShaper 1000s). A sequence of optical pulses with a repetition rate of 100 MHz and duration of 80 fs is generated by femtosecond laser (ELMO, femtosecond fiber laser). A series of pulses produced by a pulse pattern generator (Agilent, N4951A) is modulated on the optical pulse sequence, under carrier suppression situation, to reduce the repetition rate of the optical pulses. The repetition rate and duration of the RF pulses are 10 MHz and 10 ns, respectively, and the pulse peak is 1 V. Thus, the optical signal with a repetition rate of 10 MHz is generated, and the optical waveshaper is employed to edit the phase and amplitude of the input spectrum. The Vernier comb filter (VCF) is realized by a fiber Fabry–Perot interferometer (FFPI) with FSR of 10.22 GHz. The transmission peak is with the Lorentz shape, and its 3 dB bandwidth is 50 MHz. The time lens consists of an MZM and two PMs. The MZM is biased at the maximum point of the transfer function, where frequency of the RF source varies in different cases; the power of the RF source is 23 dBm. Two PMs are modulated by a single-tone signal; the frequency is twice that of the MZM. The driving power of each PM is set as 30 dBm (1 W), and 40 flat lines in amplitude frequency response within 3 dB bandwidth are obtained. More details of the lossless equalization for the frequency response of the time lens can be referred to in Ref. [20]. Theoretically, the operation bandwidth of the system is 408.8 GHz. The time lens focal dispersion can be expressed as $V_\pi/(\pi V_m \mathrm{FSR}_{\mathrm{VCF}}^2)$, where V_π is the half-wave voltage of the phase modulator, and V_m is the peak voltage of the driving signal [12]. The group delay dispersion of the time lens is exactly eliminated by the optical waveshaper with a dispersion of 9.98 ps/nm. The optical filtering centered at 193.414 THz with a bandwidth of 6 GHz is realized by an optical waveshaper (Finisar, WaveShaper 1000s). Then, the spectrally compressed signal, mixed with a reference monochromatic local laser, is coherently received by a BPD (Finisar, XPDV2120R). The linewidth of the CW laser (NKT Photonics, Koheras BASIK E15) is around 0.1 kHz. The coherence timescale (~10 ms) is much larger than the recording temporal length (~0.5 ns), so that the phase of the reference source can be considered constant during the observation window. Without this reference CW signal, the system is a time microscope, while the phase information cannot be preserved. Finally, the received signal is recorded by a real-time oscilloscope (Tektronix, MSO720004C).

The experimental results of temporal magnification for an ultrafast Gaussian pulse, with 3 dB bandwidth of 300 GHz, are illustrated in Fig. 3. The input optical pulse is estimated by numerical simulation, and its duration is around 2.9 ps. Experimentally, the optical pulse is generated by an optical waveshaper, where the pulse produced by a femtosecond laser is filtered by the optical waveshaper with a Gaussian shape of 300 GHz. The value of $\mathrm{FSR}_{\mathrm{VCF}} - \mathrm{FSR}_{\mathrm{TL}}$ is adjusted by changing the FSR of the time lens. The FSR of the time lens is set at 10.08, 10.12, and 10.17 GHz, respectively. The pulse duration is estimated by the effective width of the pulse envelope, which is obtained by downconverting the RF signal to baseband in the digital domain. When $\mathrm{FSR}_{\mathrm{VCF}} - \mathrm{FSR}_{\mathrm{TL}}$ is equal to 140 MHz, the pulse duration is stretched from the intial 2.9 ps to 0.25 ns, as shown in Fig. 3(a). When the FSR difference is equal to 100 and 50 MHz, the output temporal waveforms are, respectively, as shown in Figs. 4(b) and 4(c). Temporal magnification factors

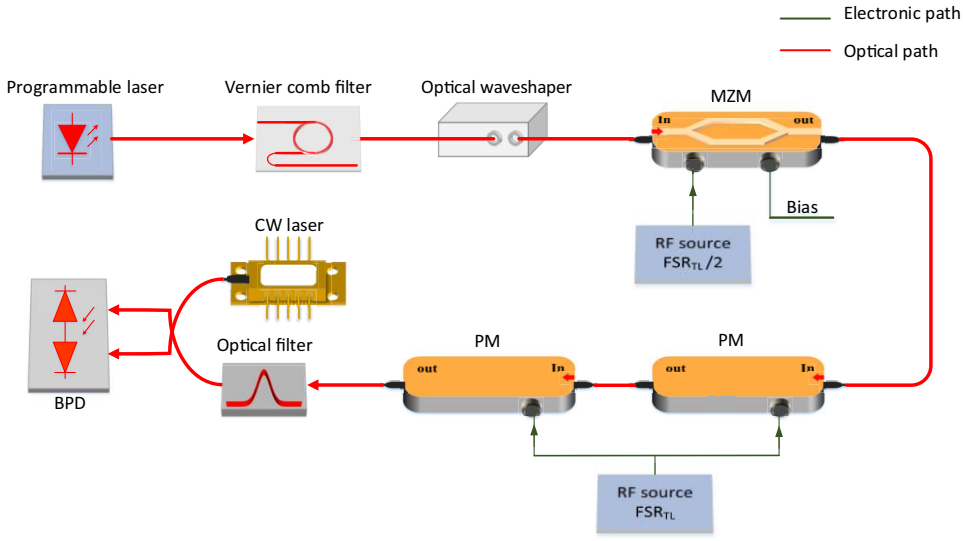

Fig. 2. Experimental setup for the real-time full-field measurements. A programmable laser is used to produce ultrafast optical signals with specific amplitude and phase characteristics. MZM, Mach–Zehnder modulator; PM, phase modulator; CW laser, continuous-wave laser; BPD, balanced photodetector. The time lens consists of an MZM and two PMs.

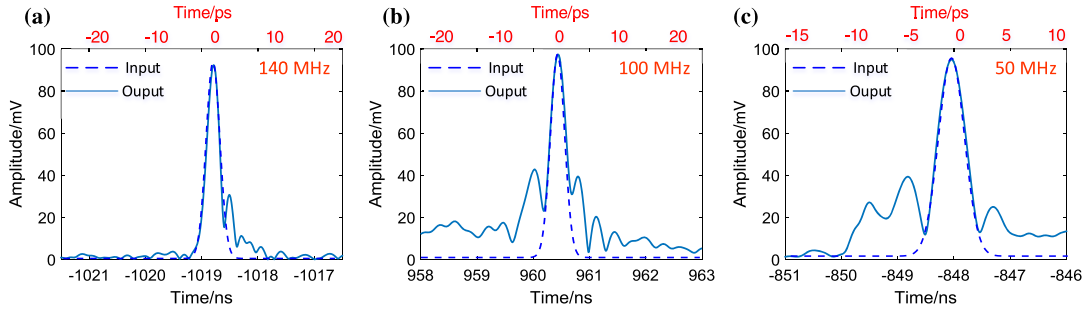

Fig. 3. Relationship between the magnification factor and the FSR difference. (a), (b), and (c), respectively, represent the output temporal waveform when $FSR_{VCF} - FSR_{TL}$ is equal to 140, 100, and 50 MHz. Dotted line: Input waveform obtained by numerical simulation. Solid line: Measured output waveform. Red horizontal is for the input waveform; black horizontal is for the output waveform.

of 102 and 224 are demonstrated, while the theoretical values are 103 and 204.4, respectively.

Real-time full-field measurements for the intensity-modulated spectrum are shown in Fig. 4. The input spectrum is generated by the femtosecond laser and optical waveshaper. The input spectrum is composed of two Gaussian shapes with 3 dB bandwidth of 40 GHz, and the frequency interval between the Gaussian peaks is 250 GHz. The phase of each Gaussian shape is linear. The numerical results of the input waveform are expressed by dotted lines in Figs. 4(a) and 4(b). Phase of the input waveform is similar to the binary phase-shift keying signal, where the phase value changes back and forth between 0 and π. In order to observe the envelope and phase of the output signal more accurately, the detected signal is downconverted into baseband through digital processing. Full-field (amplitude and phase) comparisons of the input waveform are shown in Figs. 4(a) and 4(b). When the FSR difference is 140 MHz, the original waveform with a duration of 28 ps is magnified to 2.4 ns. The temporal magnification ratio is around 86. When the FSR difference is 120 MHz, the corresponding temporal magnification ratio is around 110. The deviation value of the phase measurement is within 0.2π. Deviation of phase recovery may be caused by the uncompensated dispersion of the time lens. In general, the phase and amplitude of the input waveform are well recovered. From the view of the frequency domain, the input spectrum measured by a spectrometer (Yokogawa, AQ6370C) is shown in Fig. 4(c). When the FSR difference is set to 140 MHz, the output spectrum is shown in Fig. 4(d), and the bandwidth compression ratio is around 83. The output spectrum, corresponding to the FSR difference of 120 MHz, is shown in Fig. 4(e), and the bandwidth compression

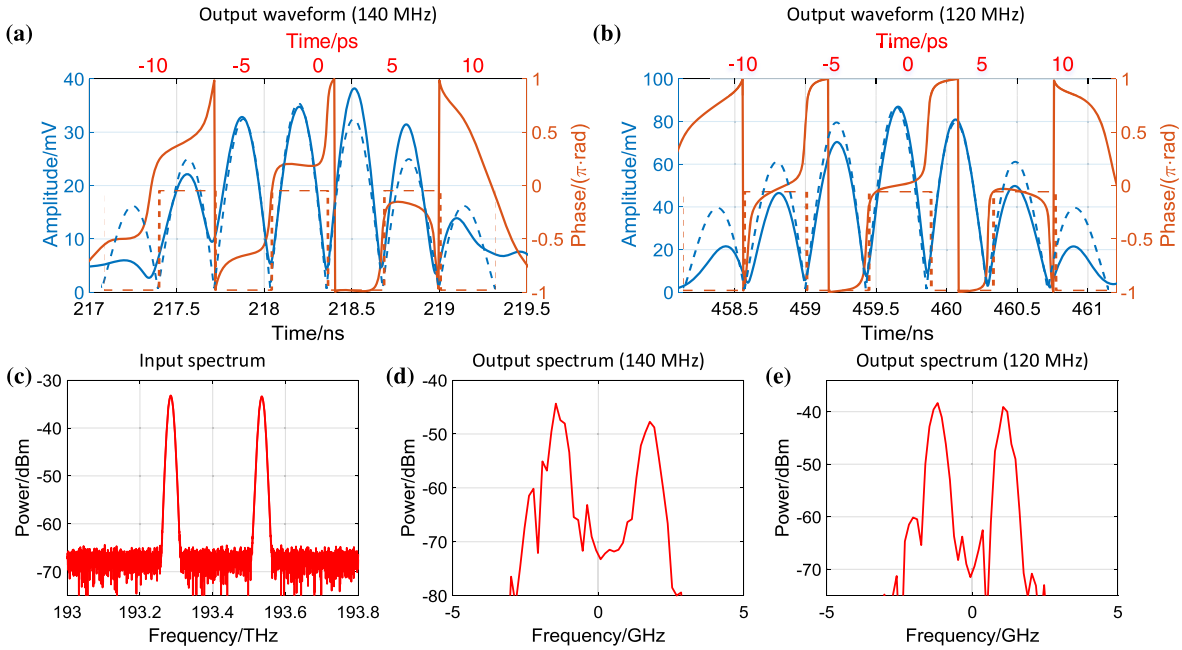

Fig. 4. Real time full-field measurements for intensity-modulated spectrum. (a) and (b), respectively, represent the comparison of the input pulse (numerical) and output pulse (measured), corresponding to the FSR difference of 140 and 120 MHz. The dotted line represents the input waveforms obtained by numerical simulation; the solid line represents the experimental results. Dark blue line: intensity of temporal waveform. Orange line: phase of temporal waveform. (c) Measured spectrum of input optical signal. (d) and (e), respectively, represent the output spectrum when the FSR difference is 140 and 120 MHz.

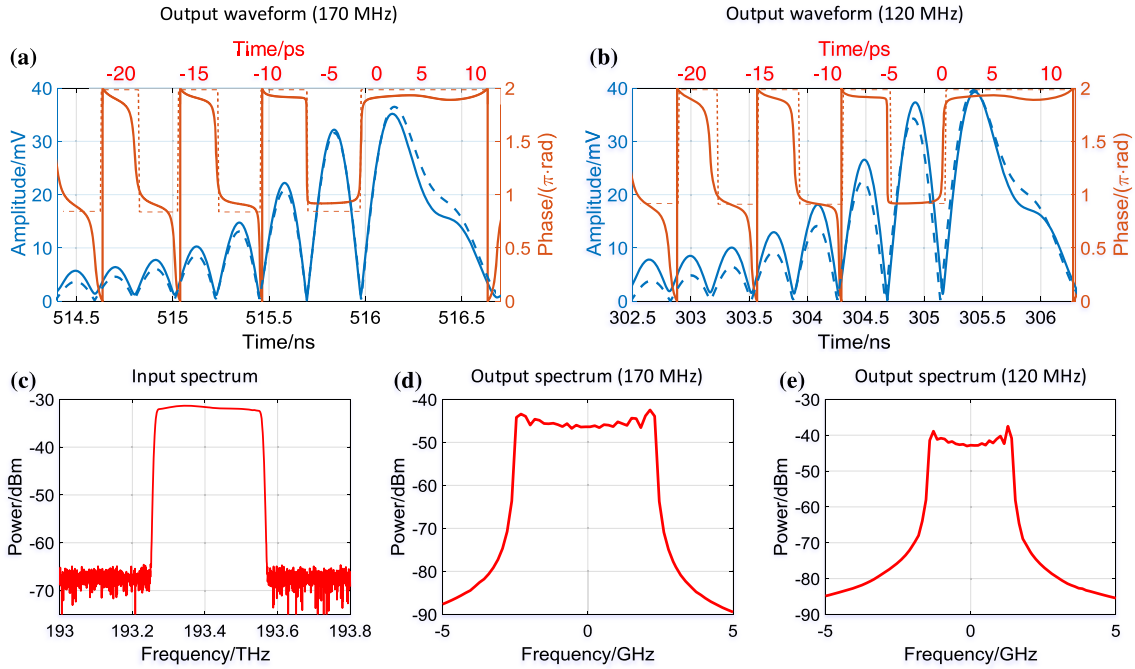

Fig. 5. Real-time full-field measurements for phase-modulated spectrum. (a) and (b), respectively, represent the comparison of the input pulse (numerical) and output pulse (measured), corresponding to the FSR difference of 170 and 120 MHz. Dotted line represents the input waveform obtained by numerical simulation; the solid line represents the experimental result. Dark blue line: the intensity of temporal waveform. Orange line: phase of temporal waveform. (c) Measured spectrum of input optical signal. (d) and (e), respectively, represent the output spectrum when the FSR difference is 170 and 120 MHz.

ratio is around 96. The bandwidth compression ratio is in good agreement with the temporal magnification factor.

In order to further verify the ability to restore the phase of an optical signal, real-time full-field measurements for a phase-modulated spectrum are performed. The bandwidth of the input spectrum is 300 GHz, and its phase characterization can be expressed as $\exp[i\pi \sin(f/60\ \text{GHz})]$. The femtosecond laser provides the ultrawide spectrum, and the following optical waveshaper edits the spectrum to acquire specific frequency characteristics. The input waveform is obtained by numerical simulation, which is represented in Figs. 5(a) and 5(b) by dotted lines. When the FSR difference is set to 170 MHz, the original pulse with a duration of 38 ps is stretched to 2.3 ns [Fig. 5(a)]. The temporal magnification ratio is around 61, while the theoretical value is 60. When the FSR difference is changed into 120 MHz, the duration of the output pulse is around 3.4 ns, and the magnification ratio is about 89 [Fig. 5(b)]. Deviation of the phase measurement is below 0.1π. The phase and amplitude of the ultrafast optical signal are well measured. The measured input spectrum is shown in Fig. 5(c). The output spectrum, corresponding to the FSR difference of 170 and 120 MHz, is, respectively, shown in Figs. 5(d) and 5(e). The bandwidth compression ratio agrees well with the theoretical analysis.

4. CONCLUSIONS

We have proposed and experimentally demonstrated real-time full-field measurements for a picosecond pulse. Different from the dispersion-based temporal magnification schemes, the proposal eliminates dependence on large dispersion. Actually, both the electro-optical modulator and periodic optical filter show great potential in integration, and the transmission delay of these optical devices is around tens of nanoseconds. Benefiting from the low latency and small volume of the existing optical device, the proposed dispersion-free scheme reduces the size of the system and improves real-time performance. Real-time full-field measurements for complex optical signals with a duration of picosecond level are experimentally demonstrated. The phase and amplitude of the ultrafast signal could be recovered without relying on complex algorithms, which may pave a new path toward the observation of transient phenomenon.

Funding. National Key Research and Development Program of China (2019YFB2203305); National Natural Science Foundation of China (62001043, 62071055); BUPT Excellent Ph.D. Students Foundation (CX2021233).

Disclosures. The authors declare no conflicts of interest.

REFERENCES

1. D. R. Solli, C. Ropers, P. Koonath, and B. Jalali, "Optical rogue waves," Nature **450**, 1054–1057 (2007).
2. J. M. Dudley, F. Dias, M. Erkintalo, and G. Genty, "Instabilities, breathers and rogue waves in optics," Nat. Photonics **8**, 755–764 (2014).
3. M. Närhi, B. Wetzel, C. Billet, S. Toenger, T. Sylvestre, J.-M. Merolla, R. Morandotti, F. Dias, G. Genty, and J. M. Dudley, "Real-time measurements of spontaneous breathers and rogue wave events in optical fibre modulation instability," Nat. Commun. **7**, 13675 (2016).

4. P. Suret, R. E. Koussaifi, A. Tikan, C. Evain, S. Randoux, C. Szwaj, and S. Bielawski, "Single-shot observation of optical rogue waves in integrable turbulence using time microscopy," Nat. Commun. **7**, 13136 (2016).
5. A. F. J. Runge, N. G. R. Broderick, and M. Erkintalo, "Observation of soliton explosions in a passively mode-locked fiber laser," Optica **2**, 36–39 (2015).
6. G. Herink, B. Jalali, C. Ropers, and D. R. Solli, "Resolving the build-up of femtosecond mode-locking with single-shot spectroscopy at 90 MHz frame rate," Nat. Photonics **10**, 321–326 (2016).
7. G. Herink, F. Kurtz, B. Jalali, D. R. Solli, and C. Ropers, "Real-time spectral interferometry probes the internal dynamics of femtosecond soliton molecules," Science **356**, 50–54 (2017).
8. P. Ryczkowski, M. Närhi, C. Billet, J.-M. Merolla, G. Genty, and J. M. Dudley, "Real-time full-field characterization of transient dissipative soliton dynamics in a mode-locked laser," Nat. Photonics **12**, 221–227 (2018).
9. X. Yi, Q.-F. Yang, K. Y. Yang, and K. Vahala, "Imaging soliton dynamics in optical microcavities," Nat. Commun. **9**, 3565 (2018).
10. B. Wetzel, A. Stefani, L. Larger, P. A. Lacourt, J. M. Merolla, T. Sylvestre, A. Kudlinski, A. Mussot, G. Genty, F. Dias, and J. M. Dudley, "Real-time full bandwidth measurement of spectral noise in supercontinuum generation," Sci. Rep. **2**, 882 (2012).
11. T. C. Wong, M. Rhodes, and R. Trebino, "Single-shot measurement of the complete temporal intensity and phase of supercontinuum," Optica **1**, 119–124 (2014).
12. R. Salem, M. A. Foster, and A. L. Gaeta, "Application of space–time duality to ultrahigh-speed optical signal processing," Adv. Opt. Photon. **5**, 274–317 (2013).
13. B. H. Kolner and M. Nazarathy, "Temporal imaging with a time lens," Opt. Lett. **14**, 630–632 (1989).
14. C. V. Bennett, R. P. Scott, and B. H. Kolner, "Temporal magnification and reversal of 100 Gb/s optical data with an up-conversion time microscope," Appl. Phys. Lett. **65**, 2513–2515 (1994).
15. V. J. Hernandez, C. V. Bennett, B. D. Moran, A. D. Drobshoff, D. Chang, C. Langrock, M. M. Fejer, and M. Ibsen, "104 MHz rate single-shot recording with subpicosecond resolution using temporal imaging," Opt. Express **21**, 196–203 (2013).
16. R. Salem, M. A. Foster, A. C. Turner-Foster, D. F. Geraghty, M. Lipson, and A. L. Gaeta, "High-speed optical sampling using a silicon-chip temporal magnifier," Opt. Express **17**, 4324–4329 (2009).
17. D. H. Broaddus, M. A. Foster, O. Kuzucu, A. C. Turner-Foster, K. W. Koch, M. Lipson, and A. L. Gaeta, "Temporal-imaging system with simple external-clock triggering," Opt. Express **18**, 14262–14269 (2010).
18. R. Salem, N. Ophir, X. Zhu, and K. Bergman, "Rapid eye diagram generation of a 640 Gb/s OTDM signal using a time lens," in *CLEO* (OSA, 2013), paper CM4G.1.
19. R. W. Gerchberg and W. O. Saxton, "A practical algorithm for the determination of the phase from image and diffraction plane pictures," Optik **35**, 237–246 (1972).
20. V. Torres-Company, J. Lancis, and P. Andrés, "Lossless equalization of frequency combs," Opt. Lett. **33**, 1822–1824 (2008).